

Experimental phase equilibria in the system $\text{LiAlSiO}_4\text{-SiO}_2\text{-H}_2\text{O}$: a petrogenetic grid for lithium-rich pegmatites

DAVID LONDON

*School of Geology and Geophysics
University of Oklahoma
Norman, Oklahoma 73019*

Abstract

Phase relations for the bulk composition $\text{LiAlSi}_5\text{O}_{12}$ (system $\text{LiAlSiO}_4\text{-SiO}_2\text{-H}_2\text{O}$) have been investigated experimentally over the range 340–950°C and 0.5–6.0 kbar $P(\text{H}_2\text{O})$. Stability relations among eucryptite, spodumene, petalite, β -spodumene (tetragonal), and virgilite (hexagonal) have been determined for quartz-saturated subsolidus conditions. The result is a quantitative P - T phase diagram that is applicable to quartz-saturated lithium aluminosilicate assemblages in pegmatites and some volcanic rocks. Thermochemical data derived from these experimental results are internally consistent and in close agreement with values obtained from calorimetry.

Under the quartz-saturated conditions that prevail in pegmatites, stability relations among the lithium aluminosilicates are a function of P and T and are largely independent of the nature and proportions of other phases in the chemically complex pegmatite system. Thus, the lithium aluminosilicate phase diagram constitutes a petrogenetic grid from which P - T conditions of emplacement and crystallization can be ascertained for many lithium aluminosilicate-bearing pegmatites.

Introduction

The lithium aluminosilicates eucryptite (Ecr: $\alpha\text{-LiAlSiO}_4$), spodumene (Spd: $\alpha\text{-LiAlSi}_2\text{O}_6$), and petalite (Pet: $\text{LiAlSi}_4\text{O}_{10}$) are valuable indicators of the conditions of magmatic and subsolidus crystallization in lithium-rich pegmatites (e.g., Stewart, 1978; London and Burt, 1982a,b,c). These three phases are the most abundant and most frequently encountered lithium minerals, so that information on their stability relations is widely applicable to a large number of pegmatitic deposits. A qualitative P - T phase diagram for the system $\text{LiAlSiO}_4\text{-SiO}_2$ offers explanations for the observed isochemical replacement of petalite by spodumene + quartz or eucryptite + quartz, and accounts for the apparent stability of eucryptite + quartz at low P and T (Burt et al., 1977; London and Burt, 1982b). Construction of a quantitative lithium aluminosilicate phase diagram has been hampered by a lack of geologically relevant experimental work and thermochemical data on phases in the system $\text{LiAlSiO}_4\text{-SiO}_2$. This paper presents a quantitative lithium aluminosilicate phase diagram that is consistent with natural occurrences of these minerals; the P - T diagram is derived from phase equilibrium experiments in siliceous portions of the system $\text{LiAlSiO}_4\text{-SiO}_2\text{-H}_2\text{O}$. The obvious value of this phase diagram for understanding lithium pegmatite petrogenesis prompted the experimental study that is reported

in this paper; some preliminary results of this work have already been published (London, 1981).

This paper focuses on the moderate- to low-temperature portion of the lithium aluminosilicate phase diagram, which is directly applicable to the petrogenesis of lithium-rich pegmatites. High-temperature portions of this diagram are relevant to phase equilibria in glass-ceramic systems (e.g., Hatch, 1943) and to some lithium-rich, high-silica volcanic rocks (e.g., the Macusani, Peru, volcanic glass: French et al., 1978).

Previous experimental work

Stability relations among the lithium aluminosilicates for quartz-saturated and undersaturated bulk compositions have been thoroughly investigated by ceramists because of the fluxing properties and low thermal expansion of lithium aluminosilicate glasses and glass-ceramics (e.g., Hatch, 1943; Roy et al., 1950; Ostertag et al., 1968). A number of experimental studies have been conducted at elevated pressures (e.g., Isaacs and Roy, 1958; Stewart, 1960, 1963, 1978; Phinney and Stewart, 1961; Edgar, 1968; Armstrong, 1969; Munoz, 1969, 1971; Drysdale, 1971, 1975; Shternberg et al., 1972; and Grubb, 1973). These studies have explained some important aspects of lithium aluminosilicate stability relations, but they do not provide a lithium aluminosilicate phase diagram that is

Table 1. Chemical analyses of starting materials*

	Eucryptite Bikita, Zimbabwe	Spodumene Nuristan, Afghanistan	Petalite Minas Gerais, Brazil USNM 149544
SiO ₂	47.92	64.39	78.37
Al ₂ O ₃	40.40	27.42	17.06
TiO ₂	<0.01	<0.01	0.02
FeO + Fe ₂ O ₃	0.08	0.24	<0.01
MnO	<0.01	<0.05	<0.01
CaO	0.09	0.06	<0.02
MgO	--	--	<0.01
K ₂ O	<0.05	<0.05	<0.01
Na ₂ O	0.05	0.16	<0.01
Li ₂ O	11.49	7.56	4.35
P ₂ O ₅	<0.01	<0.01	<0.01
H ₂ O ⁻	0.23	0.06	0.04
H ₂ O ⁺			0.09
Total	100.26	99.89	99.93

*Gravimetric and spectroscopic analyses by Joseph A. Nelen, Smithsonian Institution, Washington, DC, USA.

complete or entirely consistent with geological occurrences of these minerals (see London and Burt, 1982b, Fig. 3). Some of these studies involved only mineral syntheses in which reversible equilibrium was not demonstrated. Several studies in which reactions were reportedly reversed yielded significantly discrepant results. In particular, Stewart (1963) reported a reversal of the reaction $\text{Pet} = \text{Spd} + 2 \text{Qtz}$ at 550°C and 2 kbar $P(\text{H}_2\text{O})$, whereas Munoz (1971) gave an equilibrium temperature of 470°C at the same pressure, and D. J. Drysdale (University of Queensland, unpublished data, 1976) found that petalite is stable with respect to spodumene + quartz down to 410°C or lower at 2 kbar.

Experimental procedures

The starting materials were water-clear, inclusion-free, and colorless natural minerals: eucryptite from Bikita, Zimbabwe; spodumene from Nuristan, Afghanistan; petalite and quartz from Minas Gerais, Brazil (Table 1). Mineral grains were milled under ethanol in an agate mortar to a grain size <150 μm. Dried mineral powders were mixed to the bulk composition $\text{LiAlSi}_5\text{O}_{12}$ (e.g., 20Ecr80Qtz, in mole %) to ensure quartz saturation in subsolidus runs. Equal weight portions of the mixes 50Pet50Qtz, 25Spd75Qtz, and 20Ecr80Qtz were combined in the three possible binary combinations, so that the univariant assemblage of a given reaction was present in each capsule. Betz-spodumene and virgilite were synthesized from these mineral mixes; the synthetic phases were in turn used to establish reaction reversals. Distilled

and deionized water was used as a fluxing agent, with powder-water weight ratios maintained at about 10/1 to minimize the amount of solid material dissolved in the fluid; additional water in excess of 10 wt.% of total charge was required to produce an H₂O-saturated melt at the liquidus at 6 kbar. Charges were sealed in Pt capsules (1-cm long) for runs in water-pressurized, cold-seal reaction vessels (Tuttle, 1949); runs above 4 kbar were performed in an Ar-pressurized, internally heated, pressure vessel (Yoder, 1950). For the cold-seal system temperature was measured by external Chromel-Alumel thermocouples, and pressure was measured with a Heise bourdon tube gauge. In the internally heated vessel, temperature was measured with a Pt-Rh thermocouple, and pressure was monitored by a manganin resistance cell. Systematic errors (measured and estimated) propagated with run-time variations (imprecision) yield maximum uncertainties of ±10°C and ±100 bars for most runs. Run products were examined microscopically, by X-ray powder diffraction, and by scanning electron microscopy. Quartz in runs served as a qualitative internal standard for X-ray powder diffraction. X-ray diffraction patterns from which unit cell parameters were calculated (e.g., Table 5) were generated on a Haig-Guinier powder camera with annealed BaF₂ ($a_0 = 6.1970\text{Å}$) as internal standard. Runs above about 500°C generally went to completion, even within 10°C of univariant reaction boundaries, so that identification of the stable assemblage by X-ray powder diffraction was unambiguous; for runs below 500°C, shifts in X-ray peak intensities (integrated area) corresponding to not less than 20 vol % of reaction (by comparison with starting mineral assemblages and variable proportion mixes) were sufficient to determine the stable assemblage.

Experimental results

The lithium aluminosilicate phase diagram (Fig. 1) was constructed from run data in Table 2. Crystalline phases encountered in this system include the minerals eucryptite, spodumene, petalite, and quartz, as well as synthetic β-spodumene (tetragonal) and virgilite (hexagonal; cf. Munoz, 1969; French et al., 1978). These phases lie on the join $\text{LiAlSi}_4\text{O}_4\text{-SiO}_2$ (Fig. 1) and define an (n + 4)-phase multisystem in which seven stable subsolidus univariant reactions (Table 3) and three stable invariant points are possible for quartz-saturated bulk compositions. Three additional melting reactions that define one more invariant point were encountered at high *T* and *P* to 6 kbar. For the bulk composition used, the system is quartz-undersaturated above the solidus. Univariant boundaries for subsolidus reactions listed in Table 3 are located between bracketing runs by solution of the Clausius-Clapeyron equation $dP/dT = \Delta S^\circ/\Delta V^\circ$ and the Gibbs Free Energy equation $\Delta G^\circ = \Delta H^\circ_{\text{bar},T} - T\Delta S^\circ + (P - 1)\Delta V^\circ$. The thermodynamic solutions that were used to construct the diagram in Figure 1 are discussed in the following section.

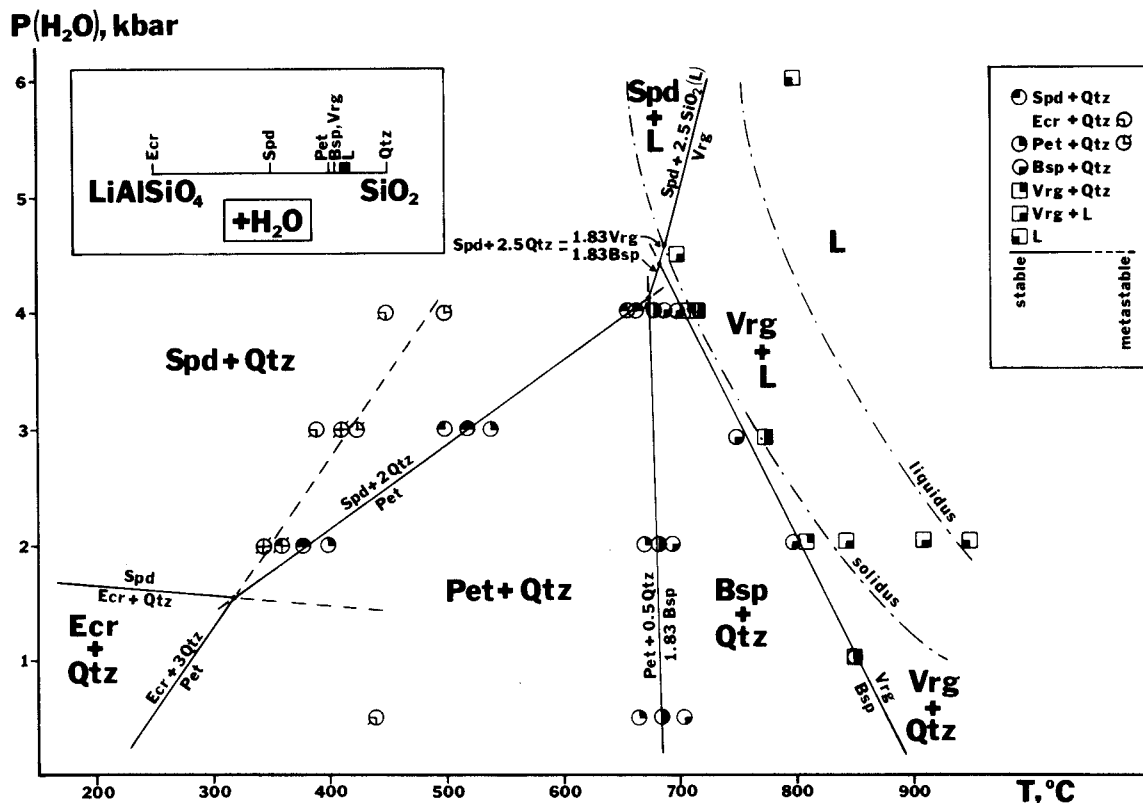


Fig. 1. Experimental pressure-temperature phase diagram for the bulk composition 20Ecr80Qtz (mole %) in the system $\text{LiAlSiO}_4\text{-SiO}_2\text{-H}_2\text{O}$. Symbols show the locations of bracketing or delimiting runs; additional runs used to define the diagram are listed in Table 2. Solid lines: stable portions of univariant reactions; dashed lines: metastable extensions; dash-dot lines: solidus and liquidus for the bulk composition $\text{LiAlSi}_5\text{O}_{12}$. Compositions of phases encountered in this study are shown on the binary $\text{LiAlSiO}_4\text{-SiO}_2$ in the upper left portion of the figure. The composition of liquid (L) is projected from H_2O ; the liquid composition varies between the eutectic composition 16Ecr84Qtz reported by Stewart (1978) and the bulk composition 20Ecr80Qtz of this study.

Spodumene-petalite relations

The univariant reaction between spodumene and petalite is located by reaction reversals at 2, 3, and 4 kbar (Fig. 1). The reaction boundary at 4 kbar lies at 660°C (cf. Stewart, 1963: 685°C at 4 kbar). Experiments at 2 kbar indicate a reaction boundary at 380°C; these results are consistent with the observations of D. J. Drysdale (unpublished data, 1976), who employed experimental procedures similar to those used in this study. The resultant slope of the reaction $\text{Pet} = \text{Spd} + 2\text{Qtz}$ (Table 3) is considerably shallower than the value reported by Stewart (1963: 23.5 bar/°C), and extends the stability field of petalite to much lower T at low P . Discrepancies in the reported experimental results of this reaction at 2 kbar (cf. Stewart, 1963; Munoz, 1971) appear to be due to differences in experimental technique. In this study, quartz saturation was maintained in all subsolidus fields. The petalite bulk composition employed by Stewart (1963) and Munoz (1971), apparently became quartz-undersaturated (i.e., shifted toward spodumene) in runs

into the petalite stability field, with the result that small amounts of spodumene would persist *stably* with petalite until the reaction $3\text{Spd} = \text{Pet} + 2\text{Ecr}$ that is terminal to spodumene was encountered at higher T . The reaction boundaries reported by Stewart (1963) and Munoz (1971) may be for the quartz-absent eucryptite-producing reaction cited above. In this regard, it is significant that Stewart's (1978) evidence for silica leaching into the aqueous phase is based in part on the appearance of small amounts of eucryptite in these runs.

In the previous experimental studies, the determination of the reaction boundary $\text{Pet} = \text{Spd} + 2\text{Qtz}$ may have been complicated further by the persistence of small amounts of Fe-rich spodumene beyond the stability field of $\alpha\text{-LiAlSi}_2\text{O}_6$. In this study, run products over a wide range of P and T contained traces (≤ 0.1 vol.%) of fine-grained ($\sim 5\ \mu\text{m}$), emerald-green, highly birefringent, lath-shaped Fe-rich spodumene. A similar phase, also identified as Fe-rich spodumene, appeared in runs performed by Stewart (pers. comm., 1980) and Munoz (pers. comm., 1982). In this study, the phase persists well into the

Table 2. Experimental run data

Reaction			
P, bars	T, °C	Duration, hours	Stable products*
<u>Pet + 0.5 Qtz = 1.83 Bsp</u>			
500	665	385	Pet + Qtz
500	685	385	Pet + Bsp + Qtz
500	707	385	Bsp + Qtz
2000	650	240	Pet + Qtz
2000	667	624	Pet + Qtz
2000	685	384	Pet + Bsp + Qtz
2000	695	624	Bsp + Qtz
2000	707	624	Bsp + Qtz
2000	730	240	Bsp + Qtz
2000	800	240	Bsp + Qtz
4000	670	599	Pet + Qtz
4000	675	95	Pet + Bsp + Qtz
4000	690	599	Bsp + Qtz
4000	695	95	Bsp + Qtz
<u>Bsp = Vrg</u>			
1000	800	24	Bsp + Qtz
1000	850	24	Bsp + Vrg + Qtz
2000	740	70	Bsp + Qtz
2000	780	240	Bsp + Qtz
2000	800	240	Bsp + Qtz
2000	810	9	Vrg + Qtz
2900	750	24	Bsp + Qtz
2900	775	24	Vrg + Qtz + L
4000	695	95	Bsp + Qtz
4000	700	66	Bsp + Qtz
4000	715	48	Vrg + Qtz
<u>Vrg + Qtz = L</u>			
2000	810	9	Vrg + Qtz
2000	845	9	Vrg + L
2000	875	9	Vrg + L
2900	775	24	Vrg + Qtz + L
4000	715	48	Vrg + Qtz + L
4500	700	48	Vrg + L
<u>Vrg = L</u>			
2000	910	24	Vrg + L
2000	950	24	L
6000	800	27	L
6000	850	24	L
6000	950	24	L
<u>Spd + 2 Qtz = Pet</u>			
2000	343	4560	Spd + Qtz
2000	360	4944	Spd + Qtz
2000	380	2952	Spd + Pet + Qtz
2000	400	2952	Pet + Qtz
2000	420	2952	Pet + Qtz
2000	440	840	Pet + Qtz
2000	480	914	Pet + Qtz

Table 2. (cont.)

Reaction			
P, bars	T, °C	Duration, hours	Stable products*
2000	520	914	Pet + Qtz
2000	560	914	Pet + Qtz
3000	460	1632	Spd + Qtz
3000	481	1632	Spd + Qtz
3000	501	1632	Spd + Qtz
3000	520	936	Spd + Pet + Qtz
3000	540	936	Pet + Qtz
3000	560	936	Pet + Qtz
4000	424	215	Spd + Qtz
4000	451	215	Spd + Qtz
4000	473	215	Spd + Qtz
4000	480	1106	Spd + Qtz
4000	520	1106	Spd + Qtz
4000	560	1106	Spd + Qtz
4000	602	616	Spd + Qtz
4000	619	600	Spd + Qtz
4000	649	600	Spd + Qtz
4000	655	137	Spd + Qtz
4000	665	137	Pet + Qtz
4000	670	599	Pet + Qtz
<u>Ecr + 3 Qtz = Pet</u>			
2000	343	4560	Pet + Ecr + Qtz
2000	360	4944	Pet + Ecr + Qtz
2000	380	2952	Pet + Qtz
2000	440	840	Pet + Qtz
2000	480	914	Pet + Qtz
2000	520	914	Pet + Qtz
2000	560	914	Pet + Qtz
3000	388	1776	Ecr + Qtz
3000	411	1776	Ecr + Qtz
3000	426	1776	Pet + Ecr + Qtz
3000	460	1632	Pet + Qtz
3000	481	1632	Pet + Qtz
3000	501	1632	Pet + Qtz
4000	450	531	Ecr + Qtz
4000	500	531	Pet + Qtz
4000	550	531	Pet + Qtz
4000	600	600	Pet + Qtz
<u>Ecr + Qtz = Spd</u>			
500	441	716	Ecr + Qtz
2000	343	4560	Spd + Qtz
2000	360	4944	Spd + Qtz
2000	380	2952	Spd + Qtz
2000	440	840	Spd + Qtz
2000	480	914	Spd + Qtz
2000	520	914	Spd + Qtz
4000	372	1488	Spd + Qtz
4000	424	1488	Spd + Qtz

*Includes products of some runs along metastable extensions of reactions Ecr + 3 Qtz = Pet and Ecr + Qtz = Spd.

petalite stability field. The Fe³⁺-spodumene also appeared in runs in which spodumene was absent from starting charges (e.g., along the metastable extension of reaction Pet = Ecr + 3 Qtz in the spodumene field). In runs that produced stable spodumene, the green phase commonly is included at the center of colorless spodumene laths. It appears that trace amounts of Fe originally present in the starting materials are partitioned into a minute amount of a spodumene phase (LiFe³⁺Si₂O₆) that lies off the LiAlSiO₄-SiO₂ join and persists well beyond

Table 3. Thermodynamic quantities of subsolidus reactions

Reaction	dP/dT, bar/K	ΔV°, J/bar	ΔS°, J/K	ΔH°, J/mol
<u>experimental</u>				
Spd = 2 Qtz = Pet	+7.5	+2.46	+18.5(16)	+6750(700)
Ecr + 3 Qtz = Pet	+14.2	+1.23	+17.4(13)	+7950(800)
Pet + 0.5 Qtz = 1.83 Bsp	-192.9	-0.28	+54.0(40)	+52000(4000)
Bsp = Vrg	-20.7	-0.04	+0.8(35)	+975(3770)
<u>calculated</u>				
Ecr + Qtz = Spd	+0.9	-1.23	-1.1(15)	+1300(800)
Spd + 2.5 Qtz = 1.83 Vrg	+35.5	+2.08	+73.9(40)	+60260(4000)
Spd + 2.5 Qtz = 1.83 Bsp	+33.1	+2.19	+72.4(40)	+60320(4000)

Table 4. Thermochemical properties of individual phases

Phase	V° , J/bar	S° , J/mol-K	ΔH_f° , J/mol
Ecr	4.797(5)	90.8(8)	-2144050(2800)
Spd	5.837(2)	131.2(9)	-3053500(2790)*
Pet	12.840(5)	232.6(9)**	-4868200(2800)
Bsp	7.470(5)	167.6(19)	-2880600(2800)
Vrg	7.428(5)	168.4(19)	-2879600(2800)
Qtz	2.2688(1)	41.46(2)*	-910700(1000)*

*from Robie *et al.* (1978)
**mean of values reported by Bennington *et al.* (1980) and Hemingway *et al.* (1983)

the stability field of α -LiAlSi₂O₆ (e.g., Appleman and Stewart, 1968). These results corroborate previous experimental evidence that iron-rich spodumene nucleates readily under hydrothermal conditions and may provide seed crystals for natural spodumene in pegmatites (Drysdale, 1975).

Eucryptite + quartz

The stability field of eucryptite + quartz lies mostly below the P - T limits of hydrothermal experimentation. Field boundaries for this assemblage were defined in part by reaction reversals along the metastable extension of the reaction $\text{Pet} = \text{Ecr} + 3 \text{Qtz}$ into the spodumene field at 3 and 4 kbar, with additionally limiting runs at 2 kbar. Most attempts to reverse the reaction $\text{Spd} = \text{Ecr} + \text{Qtz}$ metastably yielded complete reaction to (stable) petalite. The stability field of eucryptite + quartz is limited to low P and T , below about 320°C and 1.6 kbar. This observation is consistent with the rarity of the assemblage (London and Burt, 1982b, Table 2), and with the fact that eucryptite + quartz has not been identified as a primary (magmatic) assemblage.

In principle, the reaction $\text{Spd} = \text{Ecr} + 2 \text{Qtz}$ constitutes a geobarometer in that it establishes minimum pressure conditions (approximately 1.6 kbar) for the generation of spodumene pegmatites. The usefulness of this reaction, however, is limited by the fact that spodumene generally persists metastably through the eucryptite + quartz field, presumably because the boundary $\text{Spd} = \text{Ecr} + \text{Qtz}$ is encountered at such low T that retrograde reaction does not occur.

Petalite- β -spodumene

The field of petalite is bounded above 680°C by a reaction that produces tetragonal β -spodumene (Skinner and Evans, 1960; Li and Peacor, 1968). The β -spodumene so formed is more siliceous than petalite (Fig. 1 and Table 3) but does not exhibit complete solid solution with β -quartz or keatite. Skinner and Evans (1960) similarly found a miscibility gap (at >84.3 wt.% SiO₂) for β -spodumene-keatite solid solutions synthesized at one atmosphere. Unit cell parameters of tetragonal β -spodumenes synthesized in this study (Table 5) do not show a

systematic or significant variation that would reflect different phase compositions; thus the presence of excess quartz appears to fix the activity of SiO₂ in β -spodumene at a consistent and maximum value over a wide range of P and T . The location and slope of the reaction $\text{Pet} \rightarrow \text{Bsp}$ are essentially identical to values reported by Stewart (1963).

β -spodumene-virgilite transition

Beta-spodumene undergoes an isochemical transition from the keatite structure ($P4_32_12$: Skinner and Evans, 1960) to a hexagonal phase ($P6_222$: e.g., Munoz, 1969) along a negatively sloping reaction boundary. The hexagonal phase is identical to β -quartz_{ss} phases synthesized by Munoz (1969) and Stewart (1978), and to the natural analogue, virgilite, from the Macusani volcanic glass, Peru (French *et al.*, 1978). The two-phase field β -spodumene_{ss} + β -quartz_{ss} (Bsp + Vrg) that was reported by Munoz (1969) and Stewart (1978) was not encountered in this study. Instead, the subsolidus two-phase fields at high T appear to contain silica-saturated Bsp or Vrg plus essentially pure (unsubstituted) β -quartz, as evidenced by sharp X-ray powder diffraction lines for α -quartz in run products quenched from the β -quartz field plus the distinctly different lines for β -spodumene or virgilite. Under these conditions, the P - T field of β -spodumene is diminished to lower P and T . The Gibbs Free Energy change associated with reaction $\text{Bsp} = \text{Vrg}$ is extremely small (Table 6), and metastable persistence of one phase or the other might be expected in experimental runs, especially those in which H₂O (as catalyst) was absent (e.g., Munoz, 1969). Such a condition might explain Munoz' (1969) broad two-phase field of β -spodumene_{ss} + β -quartz_{ss} that expands with decreasing P and T . The results of this study agree fundamentally with Munoz' (1969) observations that tetragonal β -spodumene transforms to the hexagonal α -quartz structure with increasing P ; however, virgilite appears to be stable to pressures at least as low as 2 kbar (cf. Munoz, 1969, and Stewart, 1978).

Table 5. Unit cell parameters for β -spodumene and virgilite*

Run conditions:		Phase, Space Group		
P , bars	T , °C	a_0 , Å	c_0 , Å	V^0 , Å ³
β -spodumene, $P4_32_12$				
1000	850	7.440(3)	8.975(3)	496.7(5)
2000	730	7.443(2)	8.981(2)	497.5(3)
2000	800	7.441(2)	8.976(2)	497.0(3)
4000	690	7.438(2)	8.968(2)	496.1(3)
virgilite, $P6_222$				
2000	810	5.117(4)	5.439(4)	123.3(4)
4500	700	5.119(4)	5.440(4)	123.5(4)

*Least-squares refinement using the program of Appleman and Evans (1973); calculated direct cell error (1 σ) in parentheses.

Table 6. Gibbs Free Energy change for univariant reactions in Table 3

Spd + 2 Qtz = Pet	$\Delta G^\circ = 6750 - 18.5T + 2.46(P-1)$
Ecr + 3 Qtz = Pet	$\Delta G^\circ = 7950 - 17.4T + 1.23(P-1)$
Pet + 0.5 Qtz = 1.83 Bsp	$\Delta G^\circ = 52000 - 54.0T - 0.28(P-1)$
Bsp = Vrg	$\Delta G^\circ = 975 - 0.8T - 0.04(P-1)$
<hr/>	
Ecr + Qtz = Pet	$\Delta G^\circ = 1300 + 1.1T - 1.23(P-1)$
Spd + 2.5 Qtz = 1.83 Vrg	$\Delta G^\circ = 60260 - 73.9T + 2.08(P-1)$
Spd + 2.5 Qtz = 1.83 Bsp	$\Delta G^\circ = 60320 - 72.4T + 2.19(P-1)$

Solidus relations

As with melting relations in other alkali aluminosilicate-H₂O systems, the solidus of the lithium aluminosilicate system possesses a relatively steep negative slope that reflects substantially depressed solidus temperatures with increasing $P(\text{H}_2\text{O})$. The disappearance of quartz at the solidus in these experiments is consistent with Stewart's (1978) reported eutectic composition on the join LiAlSiO₄-SiO₂ of approximately 86.4 wt.% SiO₂ (16Ecr84Qtz, in mole %) for runs at 2 kbar $P(\text{H}_2\text{O})$. The location of this eutectic illustrates the dramatic effect of a small amount of LiAl \rightleftharpoons Si exchange on the melting temperature of quartz at 2 kbar $P(\text{H}_2\text{O})$.

Spodumene and virgilite are the stable crystalline phases in the three-phase region above the solidus (Spd or Vrg + melt + vapor). The spodumene + silica (melt) = virgilite reaction appears to have a steep positive slope (approximately +35.5 bar/°C). Extrapolation of this univariant reaction boundary to higher pressures does not yield close agreement with the results of Munoz (1969) for the isochemical spodumene = β -quartz_{ss} transition (slope = +25.6 bar/°C). Upon extrapolation to much higher P , this reaction should intersect the liquidus at another invariant point (cf. the spodumene- β -quartz_{ss}-liquid singular point at 26.5 kbar (dry), 1510°C: Munoz, 1969).

Liquidus relations

Virgilite is the only crystalline phase on the H₂O-saturated liquidus between 2 and 6 kbar $P(\text{H}_2\text{O})$. This observation strengthens the interpretation by French et al. (1978) that virgilite is a primary liquidus phase for the near-surface Macusani magma. The results of this study appear to confirm that virgilite may be stable at low pressures in subvolcanic environments; thus, the reaction Bsp = Vrg defines the minimum P - T field boundary for the pre-eruption magma at the Macusani volcanic center (cf. Noble et al., 1984). This P - T area lies in the stability field of sillimanite (Holdaway, 1971), and sillimanite has been reported from the Macusani glass (Linck, 1926).

Thermodynamic analysis

The subsolidus reaction boundaries shown in Figure 1 are located by calculation of ΔH° , ΔS° , and ΔV° for each

reaction (Table 3) by use of the Gibbs Free Energy equation and the Clausius-Clapeyron equation. Calculated values of ΔV° employ standard molar volumes of eucryptite, spodumene, petalite, and quartz (London and Burt, 1982b, Table 4), and molar volumes for β -spodumene and virgilite that are calculated from unit cell parameters of run products (Table 5). Values for ΔS° and ΔH° are calculated by solution of a system of inequalities of the form

$$\Delta H_i^\circ \text{ bar}, T - T\Delta S^\circ \geq - (P - 1)\Delta V^\circ$$

for bracketing run data (cf. Wood and Fraser, 1976, and Gordon, 1977, for methodology); this technique was used to obtain maximum and minimum values of ΔS° and ΔH° (at specified P, T , and constant ΔV°) that are constrained by bracketing runs and are consistent with all of the run data for a particular reaction. The values of ΔS° and ΔH° listed in Table 3 represent the mean of the feasible range of solutions for each thermodynamic quantity in the specific reaction. The uncertainties reported for ΔS° and ΔH° represent the maximum experimental or calculated errors and are estimated to be near $\pm 2\sigma$ for the bracketed reactions.

The experimental results alone do not allow a set of thermochemical properties for individual phases to be calculated wholly from the experimental work. Only two independent equations (reactions) relate four unknowns (phases) around each invariant point. With the input of two values for S° and ΔH_i° of crystalline phases in the system, one for each component, the thermochemical properties of the remaining crystalline phases can be calculated and compared to other sources of data. In Table 4, S° and ΔH_i° for quartz and ΔH_i° for spodumene are taken from Robie et al. (1978), and S° of petalite is the mean of calorimetric results reported by Bennington et al. (1980) and Hemingway et al. (1984). The remaining values of S° and ΔH_i° in Table 4 are generated from the tabulated molar volumes and from the thermodynamic quantities of reaction listed in Table 3.

With a value of $\Delta S^\circ = +18.5 \text{ J/mol} \cdot \text{K}$ for reaction Spd + 2 Qtz = Pet, S° for spodumene is calculated as 131.2 J/mol · K, a result that differs from the calorimetric value by less than 1.5% (Pankratz and Weller, 1967). In a similar manner, ΔS° for reaction Ecr + 3 Qtz = Pet has been used to calculate $S^\circ = 90.8 \text{ J/mol} \cdot \text{K}$ for eucryptite; for comparison, a value of $S^\circ = 90 \text{ J/mol} \cdot \text{K}$ (London and Burt, 1982b) was estimated from S° for β -eucryptite (Pankratz and Weller, 1967) corrected for ΔS° of reaction α -eucryptite = β -eucryptite (Issacs and Roy, 1958). The value of ΔH_i° for eucryptite (Table 4) differs from a similarly derived estimate (London and Burt, 1982b) by 0.28%, and the value of ΔH_i° for petalite differs from the value reported by Bennington et al. (1980) by 0.37% and lies near the 95% confidence limit for their work. These results demonstrate that the thermodynamic quantities derived from this experimental study are in close agreement with values obtained from calorimetry.

Thermochemical data derived from bracketed experiments have been used to calculate the location of three additional subsolidus reactions (Table 3). The calculated boundaries shown in Figure 1 are consistent with the limited experimental data for these reactions (Table 2). Of these three calculated boundaries, the reaction $\text{Ecr} + \text{Qtz} = \text{Spd}$ has the greatest geological relevance. This reaction is located by its intersection at the low-temperature invariant point, and by a calculated slope = $+0.9 \text{ bar}/^\circ\text{C}$. The slope of the reaction may be (+) or (-); however, the principal source of error in the location of the reaction boundary stems from the possible range of P - T locations for the invariant point, which is a function of uncertainties associated with reactions $\text{Spd} + 2 \text{ Qtz} = \text{Pet}$ and $\text{Ecr} + 3 \text{ Qtz} = \text{Pet}$. The errors in the location of the Ecr - Qtz - Spd reaction have little bearing on geological occurrences of eucryptite + quartz, in that the reaction $\text{Ecr} + \text{Qtz} = \text{Spd}$ remains highly pressure dependent and limits the field of eucryptite + quartz to low P .

All of the reactions for which ΔH has been determined are endothermic as written (Table 3); thus the reactions in which petalite breaks down to $\text{Spd} + \text{Qtz}$ or $\text{Ecr} + \text{Qtz}$ are slightly exothermic. Bennington (1982) used a value of $\Delta H_f^\circ = -4886.5 \text{ kJ/mole}$ for petalite (Bennington et al., 1980) and found that ΔH° for the reaction $\text{Pet} \rightarrow \text{Spd} + 2 \text{ Qtz}$ is a positive quantity; thus Bennington (1982) proposed that the formation of $\text{Spd} + \text{Qtz}$ from petalite should not be a spontaneous reaction with decreasing temperature, in spite of natural and experimental evidence to the contrary. This dilemma can be resolved if one accepts that ΔH° for this reaction is a small quantity ($+6.75 \text{ kJ}$ from this study), and that the discrepancies result from errors in ΔH_f° for the phases involved.

The information presented in Tables 3 and 4 and in Figure 1 elucidates some of the crystallographic relations among the lithium aluminosilicates. For example, the near-zero P - T slope of the reaction $\text{Ecr} + \text{Qtz} = \text{Spd}$ reflects a large ΔV° in conversion of the tetrahedral framework structure of eucryptite to the denser pyroxene structure of spodumene. The volume change is accompanied by changes for both Li and Al from tetrahedral to octahedral coordination. Surprisingly, ΔS° for this reaction is very small, and although the phenakite-type structure of eucryptite has not been studied in detail, the small ΔS° indicates a high degree of Li-Al-Si ordering in eucryptite (cf. Winkler, 1954; Pillars and Peacor, 1973). In contrast, the reaction $\text{Ecr} + 3 \text{ Qtz} = \text{Pet}$ is accompanied by large changes in both ΔV° and ΔS° , even though Li and Al do not undergo changes in polyhedral coordination, and the structure of petalite is fully ordered (e.g., Effenberger, 1980; Černý and London, 1983). The steep positive slopes for conversion of spodumene or petalite to β -spodumene or virgilite are related to very large changes in ΔS° for these reactions. The ΔS° values reflect sharp increases in the configurational entropy of β -spodumene and virgilite that are brought about largely by extensive disordering of Li, Al, and Si (e.g., Skinner and Evans, 1960; Li, 1968; Li and Peacor, 1968).

A petrogenetic grid for lithium-rich pegmatites

Lithium aluminosilicate stability relations around the Ecr - Spd - Pet - Qtz invariant point are particularly useful in assessing the crystallization histories of lithium-rich pegmatites. From a geological standpoint, the most important reaction in the lithium aluminosilicate system is $\text{Pet} = \text{Spd} + 2 \text{ Qtz}$, which separates the field of spodumene-bearing pegmatites from those that contain only primary petalite. The shallow P - T slope of this reaction signifies that petalite-spodumene stability relations are more pressure dependent than previous experimental work would indicate (cf. Stewart, 1963). Whether spodumene or petalite crystallizes as the primary lithium aluminosilicate phase probably depends more on depth of pegmatite emplacement than on differences in temperatures at which lithium aluminosilicate saturation occurs. These experimental results extend the stability field of petalite to relatively low T with decreasing P ; this fact helps to explain why petalite may persist upon pegmatite cooling and uplift. In numerous pegmatites, however, primary petalite exhibits partial to complete replacement by spodumene or eucryptite plus quartz; the isochemical breakdown of petalite follows from cooling through the stability field of spodumene or eucryptite or both. Eucryptite + quartz assemblages bear evidence that retrograde alteration is operative to low P and T in some lithium pegmatites. Assemblages that contain $\text{Ecr} + \text{Qtz}$ appear to be rare, but five of the nine reported occurrences of this assemblage are from the largest known rare-metal pegmatite deposits (London and Burt, 1982b, Table 2); the presence of eucryptite + quartz may have significance for economic evaluation of pegmatitic deposits.

The stability field of the zeolite bikitaite ($\text{LiAlSi}_2\text{O}_6 \cdot \text{H}_2\text{O}$) was not investigated experimentally, and the phase did not appear in any runs. On the basis of synthesis and decomposition studies (Phinney and Stewart, 1961; Drysdale, 1971), bikitaite appears to be stable at low P and T . At the Bikita pegmatite, Zimbabwe, bikitaite forms by replacement of $\text{Ecr} + \text{Qtz}$ (Hurlbut, 1957); this reaction relationship indicates a very low P - T field for bikitaite. Eucryptite-bikitaite-quartz stability relations are dependent also on the activity of H_2O , as seen from the reaction $\text{LiAlSiO}_4 + \text{SiO}_2 + \text{H}_2\text{O} = \text{LiAlSi}_2\text{O}_6 \cdot \text{H}_2\text{O}$. Thus, a decrease in activity of H_2O (as, for example, by the generation of a CO_2 -rich fluid) enhances the stability of $\text{Ecr} + \text{Qtz}$.

Reactions involving petalite or eucryptite bound the stability field of spodumene + quartz at moderate to low P , but the field of $\text{Spd} + \text{Qtz}$ is unbounded at high P except by melting reactions (e.g., Munoz, 1969). Estimates of fluid inclusion entrapment conditions, however, generally place the formation of primary spodumene in the range of 3–5 kbar and 500–650°C (e.g., Bazarov, 1976; Makagon et al., 1978; London et al., 1982). Late-stage or secondary spodumene in miarolytic cavities or Alpine-type fissure veins (e.g., Hiddentite, North Carolina)

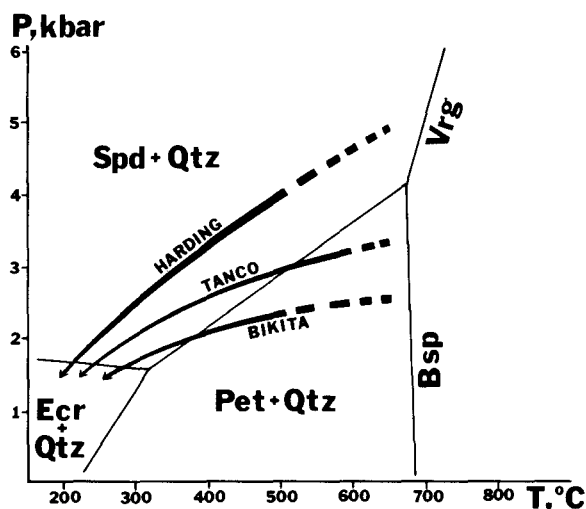


Fig. 2. Inferred P - T crystallization paths for the Harding, Tanco, and Bikita pegmatites, as defined by lithium aluminosilicate + quartz assemblages at these deposits.

probably crystallizes near the low P - T portion of the Spd + Qtz field. Nucleation and growth of spodumene at such low P and T may be aided by $(\text{Fe,Cr})^{3+} \rightleftharpoons \text{Al}^{3+}$ substitutions (Brown, 1971; Drysdale, 1975).

The stability fields of spodumene and petalite are bounded at 675–700°C by β -spodumene (below 4.4 kbar) and virgilite (above 4.4 kbar). The absence of β -spodumene or virgilite in pegmatites apparently signifies that such Li-rich magmas become saturated with respect to lithium aluminosilicates below about 700–675°C, and possibly well below these temperatures. Mineral assemblages of metamorphic rocks that host spodumene- or petalite-bearing pegmatites may not be generally usable in establishing the conditions of pegmatite crystallization, because the generation and emplacement of pegmatite magmas usually postdates the development of prograde metamorphism (Černý, 1982). Mineral assemblages of host rocks in equilibrium with lithium-rich magmas should be indicative of the upper greenschist-lower amphibolite facies (cf. Moody et al., 1983) and in the vicinity of the aluminosilicate triple point (Holdaway, 1971).

At some economically significant pegmatites (e.g., Harding, New Mexico; Bikita, Zimbabwe; Tanco, Manitoba; Londonderry, Western Australia), two or all three of the pegmatitic lithium aluminosilicates occur together with quartz. In these important cases, the lithium aluminosilicate phase diagram can be used to establish reasonably well constrained P - T crystallization paths from magmatic to subsolidus conditions. Inferred P - T paths for the Harding, Tanco, and Bikita pegmatites are shown in Figure 2. The crystallization paths are roughly defined by lithium aluminosilicate assemblages that are reported from these pegmatites (Hurlbut, 1962; Cooper, 1964; Černý and Ferguson, 1972; Černý, 1975; Jahns and Ewing, 1976; London and Burt, 1982b). The path for the Tanco pegmatite is delineated further by studies of fluid

inclusions in lithium aluminosilicates and associated quartz (London, 1982; 1983; London et al., 1982). Paths for the Harding and Bikita pegmatites are only approximations, but they are being similarly evaluated by fluid inclusion studies. The paths illustrated in Figure 2 indicate that primary crystallization and subsequent retrograde alteration in these pegmatites span a broad P - T interval. Inasmuch as retrograde alteration appears to be operative to low P and T , lithium-rich pegmatites may crystallize and recrystallize over relatively long periods of time.

It is important to note that under the quartz-saturated conditions that prevail in pegmatites, stability relations among the lithium aluminosilicates are a function of P and T and are largely independent of the nature and proportions of other phases in the chemically complex pegmatite system. Thus, lithium aluminosilicate phase relations can be used to ascertain P - T conditions within individual pegmatites (as in Fig. 2), or the regional P - T conditions of a pegmatite field (where lithium aluminosilicates are present). The lithium aluminosilicate phase diagram serves as a frame of reference for evaluation of other pegmatitic phenomena, such as metasomatic replacements, rare-element ore deposition, and the nature of the magmatic to hydrothermal transition in lithium-rich pegmatites.

Acknowledgments

Special thanks to D. M. Burt (Arizona State University), whose initial insight and guidance led to this experimental investigation, and to H. S. Yoder, Jr. (Geophysical Laboratory) for additional support. D. B. Stewart (U. S. Geological Survey), J. L. Munoz (University of Colorado), and D. J. Drysdale (University of Queensland) graciously provided unpublished data pertinent to this study. H. W. Day, D. A. Hewitt, B. O. Mysen, D. B. Stewart, and H. S. Yoder, Jr. provided thorough and constructive reviews of the manuscript. J. A. Nelen (Smithsonian Institution) performed chemical analyses of the starting materials; G. Speicher (Geophysical Laboratory) provided technical assistance; C. A. Francis and C. S. Hurlbut (Harvard University) supplied the eucryptite starting material.

Funding was provided by NSF Grant #EAR-7814785 (to D. M. Burt, Arizona State University, 1980–1982), by a postdoctoral fellowship from the Carnegie Institution of Washington (1982–1983), and by a grant from the Oklahoma Mining and Mineral Resources Research Institute. Most of the experimental work was performed at the Geophysical Laboratory, Washington, D.C., and at the U. S. Geological Survey, Reston, Virginia.

References

- Appleman, D. E. and Evans, H. T., Jr. (1973) Indexing and least-squares refinement of powder diffraction data. U. S. Geological Survey Computer Contribution 20 (Available through National Technical Information Service, file no. USGS-GD-73-003).
- Appleman, D. E. and Stewart, D. B. (1968) Crystal chemistry of spodumene-type pyroxenes. (abstr.) Geological Society of America Special Paper, 101, 5–6.
- Armstrong, C. W. (1969) The role of replacement processes in the formation of complex lithium pegmatites. Unpublished Ph.D. dissertation, University of Ontario, London, Canada.

- Bazarov, L. S. (1976) Physico-chemical conditions of crystallization of the rare-metal granitic pegmatites [in Russian]. In Dolgov, Yu. A., Ed., *Genetic Studies in Mineralogy*. Novosibirsk Institute of Geology and Geophysics, Siberian Branch of the Academy of Sciences of the USSR 94–101 (English translation of author's abstract in Roedder, E., and Kozlowski, A., Eds. (1977) *Fluid Inclusion Research: Proceedings of COFFI*, 10, 20).
- Bennington, K. O. (1982) Stability relations between petalite ($\text{LiAlSi}_4\text{O}_{10}$) and spodumene ($\text{LiAlSi}_2\text{O}_6$). U.S. Bureau of Mines Reports of Investigation, 8719.
- Bennington, K. O., Stuve, J. M., and Ferrante, M. J. (1980) Thermodynamic properties of petalite ($\text{Li}_2\text{Al}_2\text{Si}_8\text{O}_{20}$). U.S. Bureau of Mines Reports of Investigations, 8451.
- Brown, W. L. (1971) On lithium and sodium trivalent-metal pyroxenes and crystal field affects. *Mineralogical Magazine*, 38, 43–48.
- Burt, D. M., London, D., and Smith, M. R. (1977) Eucryptite from Arizona, and the lithium aluminosilicate phase diagram. (abstr.) *Geological Society of America Abstracts with Programs*, 9(7), 917.
- Černý, P. (1975) Granitic pegmatites and their minerals: selected examples of recent progress. *Fortschritte der Mineralogie, Special Volume 52* (Papers and Proceedings of the 9th General Meeting of the International Mineralogical Association, 1974), 225–250.
- Černý, P. (1982) Petrogenesis of granitic pegmatites. In P. Černý, Ed., *Granitic Pegmatites in Science and Industry*. Mineralogical Association of Canada Short Course Handbook, 8, 405–461.
- Černý, P. and Ferguson, R. B. (1972) Petalite and spodumene relations. *Canadian Mineralogist*, 11, 660–678.
- Černý, P. and London, D. (1983) Crystal chemistry and stability of petalite. *Tschermak's mineralogische und petrographische Mitteilungen*, 31, 81–96.
- Cooper, D. G. (1964) The geology of the Bikita pegmatite. In S. H. Haughton, Ed., *The Geology of Some Ore Deposits in Southern Africa*, Geological Society of South Africa, 2, 441–461.
- Drysdale, D. J. (1971) A synthesis of bikitaite. *American Mineralogist*, 56, 1718–1723.
- Drysdale, D. J. (1975) Hydrothermal synthesis of various spodumenes. *American Mineralogist*, 60, 105–110.
- Edgar, A. D. (1968) The α - β - $\text{LiAlSi}_2\text{O}_6$ (spodumene) transition from 5000 to 45000 lb/in² $P_{\text{H}_2\text{O}}$. In *International Mineralogical Association, Papers and Proceedings, 5th General Meeting*, p. 222–231. Cambridge, England, 1966, Mineralogical Society, London.
- Effenberger, H. (1980) Petalite, $\text{LiAlSi}_4\text{O}_{10}$: Verfeinerung der Kristallstruktur, Diskussion der Raumgruppe und Infrarot-Messung. *Tschermak's mineralogische und petrographische Mitteilungen*, 27, 129–142.
- French, B. M., Jazek, P. A., and Appleman, D. E. (1978) Virgilite, a new lithium aluminum silicate mineral from the Macusani glass, Peru. *American Mineralogist*, 63, 461–465.
- Gordon, T. (1977) Derivation of internally consistent thermochemical data from phase equilibrium experiments using linear programming. In H. J. Greenwood, Ed., *Application of Thermodynamics to Petrology and Ore Deposits*, Mineralogical Association of Canada Short Course Handbook, 2, 185–198.
- Grubb, P. L. C. (1973) Paragenesis of spodumene and other lithium minerals in some Rhodesian pegmatites. In *Symposium on Granites, Gneisses and Related Rocks*, Geological Society of South Africa, 3, 201–216.
- Hatch, R. A. (1943) Phase equilibrium in the system $\text{Li}_2\text{O}-\text{Al}_2\text{O}_3-\text{SiO}_2$. *American Mineralogist*, 28, 471–496.
- Hemingway, B. S., Robie, R. A., Kittrick, J. A., Grew, E. S., Nelen, J. A., and London, D. (1984) The heat capacities of osumilite from 298.15 to 1000 K, the thermodynamic properties of two natural chlorites to 500 K, and the thermodynamic properties of petalite to 1800 K. *American Mineralogist*, 69, 701–710.
- Holdaway, M. J. (1971) Stability of andalusite and the aluminosilicate phase diagram. *American Journal of Science*, 271, 97–131.
- Hurlbut, C. S., Jr. (1957) Bikitaite, $\text{LiAlSi}_2\text{O}_6 \cdot \text{H}_2\text{O}$, a new mineral from Southern Rhodesia. *American Mineralogist*, 42, 792–797.
- Hurlbut, C. S., Jr. (1962) Data on eucryptite from Bikita, Southern Rhodesia. *American Mineralogist*, 47, 557.
- Isaacs, T. and Roy, R. (1958) The α - β inversions of eucryptite and spodumene. *Geochimica et Cosmochimica Acta*, 15, 213–217.
- Jahns, R. H. and Ewing, R. C. (1976) The Harding Mine, Taos County, New Mexico. *New Mexico Geological Society Guidebook, 27th Field Conference*, Vermejo Park, 263–276.
- Li, C.-T. (1968) The crystal structure of $\text{LiAlSi}_2\text{O}_6$ -III (high quartz solid solution). *Zeitschrift für Kristallographie*, 127, 327–348.
- Li, C.-T. and Peacor, D. R. (1968) The crystal structure of $\text{LiAlSi}_2\text{O}_6$ -II (“ β -spodumene”). *Zeitschrift für Kristallographie*, 126, 46–65.
- Linck, G. (1926) Ein neuer kristallführender Tektit von Paucartambo in Peru. *Chemie die Erde*, 2, 157–174.
- London, D. (1981) Preliminary experimental results in the system $\text{LiAlSiO}_4-\text{SiO}_2-\text{H}_2\text{O}$. *Carnegie Institution of Washington Year Book*, 80, 341–345.
- London, D. (1982) Fluid–solid inclusions in spodumene from the Tanco pegmatite, Bernic Lake, Manitoba. (abstr.) *Geological Society of America Abstracts with Programs*, 14(7), 549.
- London, D. (1983) The magmatic-hydrothermal transition in rare-metal pegmatites: fluid inclusion evidence from the Tanco mine, Manitoba. (abstr.) *Transactions of the American Geological Union*, 64 (45), 549.
- London, D. and Burt, D. M. (1982a) Alteration of spodumene, montbrasite, and lithiophilite in pegmatites of the White Picacho district, Arizona. *American Mineralogist*, 67, 97–113.
- London, D. and Burt, D. M. (1982b) Lithium aluminosilicate occurrences in pegmatites and the lithium aluminosilicate phase diagram. *American Mineralogist*, 67, 483–493.
- London, D. and Burt, D. M. (1982c) Chemical models for lithium aluminosilicate stabilities in pegmatites and granites. *American Mineralogist*, 67, 494–509.
- London, D., Spooner, E. T. C., and Roedder, E. (1982) Fluid–solid inclusions in spodumene from the Tanco pegmatite, Bernic Lake, Manitoba. *Carnegie Institute of Washington Year Book*, 81, 334–339.
- Makagon, V. M., Tauson, L. S., and Kuz'mina, T. M. (1978) Physicochemical conditions of pegmatite formation with different ore specialization in Eastern Siberia [in Russian]. (abstr.) *Thermobarogeochemistry in Geology*, 1, 54–55 (English translation of author's abstract in Roedder, E., and Kozlowski, A., Eds., *Fluid Inclusion Research: Proceedings of COFFI*, 11, 130–131).

- Moody, J. B., Meyer, D., and Jenkins, J. E. (1983) Experimental characterization of the greenschist–amphibolite boundary in mafic systems. *American Journal of Science*, 283, 48–92.
- Munoz, J. L. (1969) Stability relations of $\text{LiAlSi}_2\text{O}_6$ at high pressure. *Mineralogical Society of America Special Paper* 2, 203–209.
- Munoz, J. L. (1971) Hydrothermal stability relations of synthetic lepidolite. *American Mineralogist*, 56, 2069–2087.
- Noble, D. C., Vogel, T. A., Peterson, P. S., Landis, G. P., Grant, N. K., Jazek, P. A., and McKee, E. H. (1984) Rare-element-enriched, S-type ash-flow tuffs containing phenocrysts of muscovite, andalusite, and sillimanite, southeastern Peru. *Geology*, 12, 35–39.
- Ostertag, W., Fischer, G. R., and Williams, J. P. (1968) Thermal expansion of synthetic β -spodumene and β -spodumene-silica solid solution. *Journal of the American Ceramic Society*, 51, 651–654.
- Pankratz, L. B. and Weller, W. W. (1967) Thermodynamic properties of three lithium aluminosilicates. U. S. Bureau of Mines Reports of Investigations, 7001.
- Phinney, W. W. and Stewart, D. B. (1961) Some physical properties of bikitaite and its dehydration and decomposition products. U. S. Geological Survey Professional Paper, 424, D353–357.
- Pillars, W. W. and Peacor, D. R. (1973) The crystal structure of beta eucryptite as a function of temperature. *American Mineralogist*, 58, 681–690.
- Robie, R. A., Hemingway, B. S., and Fisher, J. R. (1978) Thermodynamic properties of minerals and related substances at 298.15K and 1 bar (10^5 Pascals) pressure and at higher temperatures. U. S. Geological Survey Bulletin, 1452.
- Roy, R., Roy, D. M., and Osborn, E. F. (1950) Compositional and stability relationships among the lithium aluminosilicates: eucryptite, spodumene, and petalite. *Journal of the American Ceramic Society*, 33, 152–159.
- Shternberg, A. A., Ivanova, T. N., and Kuznetsov, V. A. (1972) Spodumene—a mineral depth indicator. *Doklady Akademii Nauk SSSR*, 202, 175–178 (transl. Proceedings of the Academy of Sciences, USSR, Earth Science Sections, 202, 111–114, 1973).
- Skinner, B. J. and Evans, H. T. (1960) β -spodumene solid solutions and the join $\text{Li}_2\text{O}-\text{Al}_2\text{O}_3-\text{SiO}_2$. *American Journal of Science*, 258A, 312–324.
- Stewart, D. B. (1960) The system $\text{LiAlSiO}_4-\text{NaAlSi}_3\text{O}_8-\text{H}_2\text{O}$ at 2000 bars. *International Geological Congress, XXI Session, Part 17*, 15–30.
- Stewart, D. B. (1963) Petrogenesis and mineral assemblages of lithium-rich pegmatites. (abstr.) *Geological Society of American Special Papers*, 76, 159.
- Stewart, D. B. (1978) Petrogenesis of lithium-rich pegmatites. *American Mineralogist*, 63, 970–980.
- Tuttle, O. F. (1949) Two pressure vessels for silicate-water studies. *Geological Society of American Bulletin*, 60, 1727–1729.
- Winkler, H. G. F. (1954) Struktur und polymorphie des eukryptits (tief- LiAlSiO_4). *Heidelberger Beiträge zur Mineralogie und Petrographie*, 4, 233–242.
- Wood, B. J. and Fraser, D. G. (1976) *Elementary Thermodynamics for Petrologists*. Oxford University Press, Great Britain.
- Yoder, H. S., Jr. (1950) High-low quartz inversion up to 10,000 bars. *Transactions of the American Geophysical Union*, 31, 827–835.

*Manuscript received, July 28, 1983;
accepted for publication, May 29, 1984.*